Actin behavior in bulk cytoplasm is cell cycle regulated in early vertebrate embryos

Christine M. Field[1,2,*], Martin Wühr[2], Graham A. Anderson[1,3], Hao Yuan Kueh[4], Devin Strickland[1,5] and Timothy J. Mitchison[1,2]

[1]Marine Biological Laboratory, Woods Hole, MA 02543, USA
[2]Department of Systems Biology, Harvard Medical School, Boston, MA 02115, USA
[3]Department of Chemical and Systems Biology, Stanford University School of Medicine, Stanford, CA 94305-5174, USA
[4]California Institute of Biology, Division of Biology, 1200 East California Blvd, Pasadena, CA 91125, USA
[5]Department of Biochemistry and Molecular Biology, University of Chicago, 929 East 57th Street, Chicago, IL 60637, USA
*Author for correspondence (christine_field@hms.harvard.edu)

Accepted 2 February 2011
Journal of Cell Science 124, 2086-2095

doi:10.1242/jcs.082263

Summary

The mechanical properties of cells change as they proceed through the cell cycle, primarily owing to regulation of actin and myosin II. Most models for cell mechanics focus on actomyosin in the cortex and ignore possible roles in bulk cytoplasm. We explored cell cycle regulation of bulk cytoplasmic actomyosin in *Xenopus* egg extracts, which is almost undiluted cytoplasm from unfertilized eggs. We observed dramatic gelation-contraction of actomyosin in mitotic (M phase) extract where Cdk1 activity is high, but not in interphase (I-phase) extract. In spread droplets, M-phase extract exhibited regular, periodic pulses of gelation-contraction a few minutes apart that continued for many minutes. Comparing actin nucleation, disassembly and myosin II activity between M-phase and I-phase extracts, we conclude that regulation of nucleation is likely to be the most important for cell cycle regulation. We then imaged F-actin in early zebrafish blastomeres using a GFP–Utrophin probe. Polymerization in bulk cytoplasm around vesicles increased dramatically during mitosis, consistent with enhanced nucleation. We conclude that F-actin polymerization in bulk cytoplasm is cell cycle regulated in early vertebrate embryos and discuss possible biological functions of this regulation.

Key words: Actin, Actomyosin, Embryo, Cell cycle

Introduction

Animal cells change in shape and stiffness as they proceed through the cell cycle. In culture, cells typically round up during mitosis, cleave during cytokinesis and spread out as they re-enter interphase (reviewed in Kunda and Baum, 2009). Eggs and blastomeres in early embryos undergo comparable shape changes, rounding and stiffening during mitosis and cytokinesis and relaxing during interphase (Mitchison and Swan, 1955; Hara et al., 1980), as do cells in epithelia (Gibson et al., 2006). Most models for cell-cycle-regulated shape change posit that the driving force comes from the cell cortex, where F-actin and myosin II interact to generate cortical tension (Bray and White, 1988). Increased cortical tension, regulated by RhoA, is thought to drive mitotic rounding in cultured cells (Maddox and Burridge, 2003), although decreased adhesion due to turning off of Rap1 is also important (Dao et al., 2009). Focused cortical tension is thought to drive ingression of the cleavage furrow (Schroeder, 1968) (reviewed by Eggert et al., 2006). These models do not consider possible mechanical contributions from bulk cytoplasm in cell-cycle-regulated shape change.

F-actin and myosin II are present in bulk cytoplasm in both somatic cells and early embryos, where they might contribute to cell mechanics. However, historically they have been difficult to image. A strong signal from the cortex tends to obscure signal from bulk cytoplasm in fluorescence microscopy of actomyosin in small somatic cells, whereas imaging deep in large embryonic cells is challenging. One solution is to investigate actin dynamics in cell and embryo extracts. A common phenomenon observed in early extract studies was gelation-contraction, where bulk actin polymerizes, gels into a cross-linked filament network and then contracts under the influence of myosin II. This was one of the founding observations for the field of non-muscle cell motility, and investigation of its mechanism led to the purification of important actin-interacting proteins (Pollard, 1981). Gelation-contraction was recently reconstituted from pure mixtures of actin, a filament cross-linker and myosin II (Bendix et al., 2008). Cell cycle regulation of gelation-contraction in extracts has not, to our knowledge, been previously studied.

Xenopus egg extract provides a useful system for investigating cell cycle regulation of cytoskeletal dynamics. It is essentially undiluted cytoplasm, where the cell cycle state can be controlled using physiological regulators. It contains abundant organelles and supports vigorous energy metabolism through respiration and glycolysis (Niethammer et al., 2008). Cell cycle regulation of the microtubule cytoskeleton has been intensively investigated in *Xenopus* egg extract (Belmont et al., 1990; Verde et al., 1992) but cell cycle regulation of actomyosin has not. Mitotic (M-phase) extract tends to undergo gelation-contraction upon warming to room temperature (Murray and Kirschner, 1989; Desai et al., 1999). For this reason, cytochalasin D has been routinely added to inhibit actin assembly when studying mitosis in this system. Actin–microtubule interactions have been investigated in interphase (I-phase) extract, revealing motor-dependent interactions (Waterman-Storer et al., 2000). However, cell cycle regulation of actin and myosin II has not been systematically investigated in this system. Here, we report strong cell cycle regulation of the bulk behavior of actomyosin in egg extracts, investigate its mechanism and go on to show that similar behavior occurs in living zebrafish embryos.

Journal of Cell Science

Results

M-phase egg extract exhibits periodic waves of gelation-contraction

M-phase extracts prepared from unfertilized eggs in the absence of cytochalsin initiated gelation-contraction within 0.5–2 minutes of warming to room temperature. This was observed by formation of a macroscopic contracted gel in microfuge tubes (Fig. 1A). We developed several formats for following this contraction by low-magnification microscopy (Fig. 1B). In drops under oil, contraction of particulates to a spot in the center was easily followed by dark-field microscopy (Fig. 1C). The lipophilic dyes DiOC6 and DiC18, which predominantly stain mitochondria and ER, respectively, in the extract system (T.J.M., unpublished), stained the central spot brightly (data not shown), indicating most organelles are now concentrated in the center of the drop. Formation of the organelle-rich contracted gel was inhibited by addition of 3 μg/ml cytochalsin D (data not shown) indicating an essential role for actin polymerization.

When M-phase extract was observed at higher magnification in the sandwich-format, multiple waves of gelation-contraction were observed. Fig. 1D and supplementary material Movie 1 show typical examples. Successive waves of contracting gel moved inwards at rates of 100–600 μm per minute. Movement rates seemed to depend upon the geometry, as well as the method of

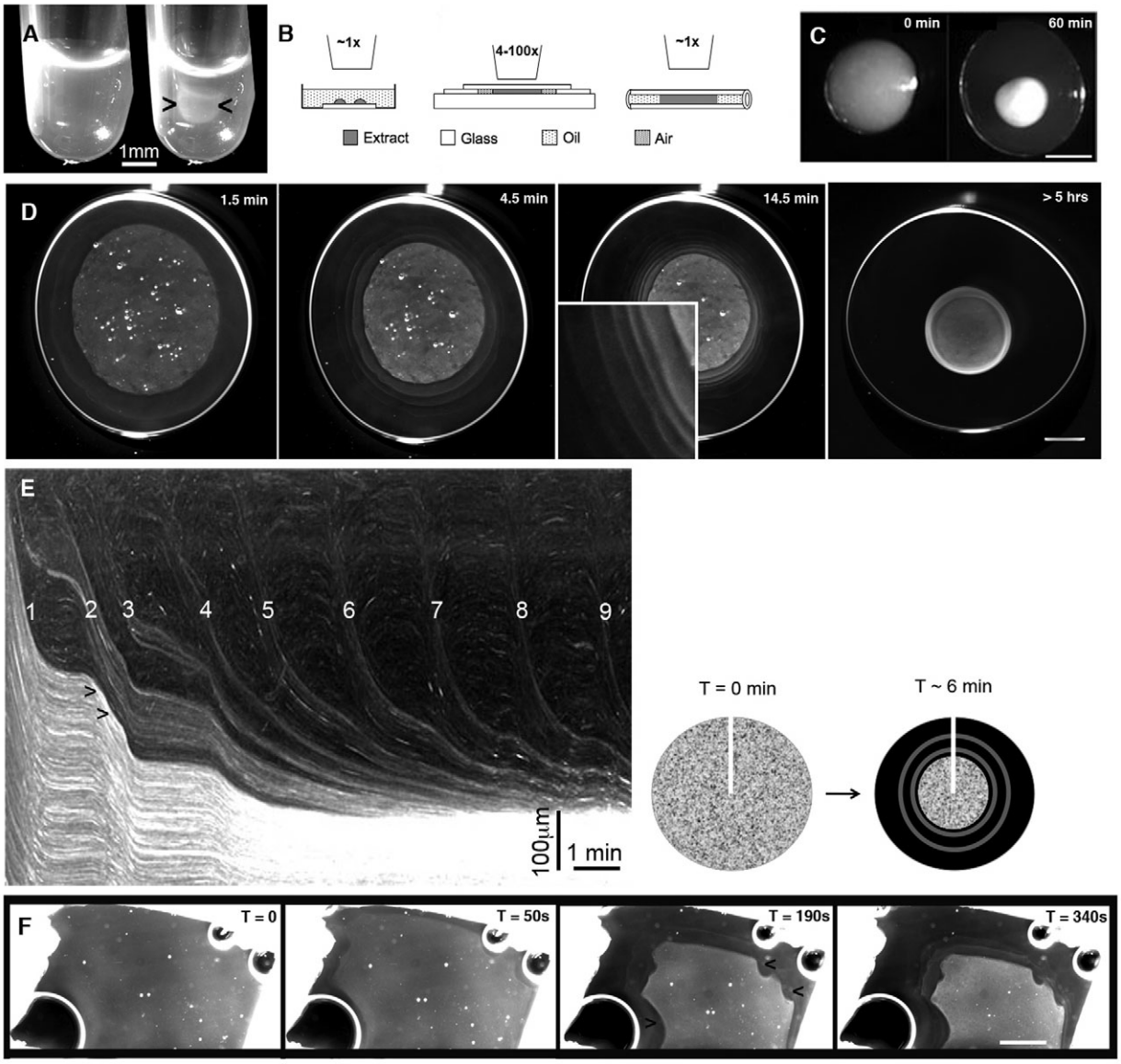

Fig. 1. Gelation-contraction in M-phase *Xenopus* egg extract. (**A**) M-phase extract in a microfuge tube before (left) and after (right) incubation at room temperature for 60 minutes. Chevrons indicate contracted gel. (**B**) Schematic of imaging configurations. In order from the left: drop under oil, sealed sandwich, and tube or capillary. (**C**) Gelation-contraction of an aliquot (1 μl) of M-phase extract in drop format. (**D**) Waves of gelation-contraction (dark-field illumination, sandwich format). The inset in the third panel is 4× magnification. (**E**) Kymograph analysis of waves. The thick white line in the schematic on the right-hand side indicates the thin radial slice copied from each frame to create the kymograph. Time is on the *x*-axis and distance is on the *y*-axis. Numbers in white indicate the wave number. Chevrons in black indicate a point where wave 1 speeds up after a being impacted by wave 2. The initial rate of ingression of the first wave is ~520 μm per minute. (**F**) Gelation-contraction in a rectangular chamber. Bubbles in the chamber create concavities. Note the preservation of shape at the edge as the gel contracts (e.g. chevrons at 190 seconds). All times are time (T) elapsed from warming to room temperature in minutes. Scale bars: 1 mm (A,F); 500 μm (C); 600 μm (D).

extract preparation, and were variable between experiments, but similar for successive waves in the same squash. Waves of organelle-rich gel piled up around the contracted core, where they were visible as a series of bright concentric circles by dark-field microscopy (Fig. 1D, inset in the third panel).

To obtain more detailed information on gel movement kinetics, we plotted kymographs of the contracting waves imaged by dark-field microscopy (Fig. 1E). A thin radial slice is copied from each frame of a dark-field time-lapse movie (indicated by the thick white line in the schematic on the right-hand side of Fig. 1E) and arranged side-by-side from left to right. This kymograph allowed comparison of nine successive waves of gelation-contraction. Successive waves moved inwards at similar rates (the more vertical the trace, the faster the rate). They slowed as they neared the core, but a stalled wave transiently increased its speed again when the subsequent wave moved inwards (see arrowheads). This observation suggests successive waves are mechanically coupled, at least near the center of the droplet. Thus an incoming wave is able to compress a wave that has already contracted.

Periodic gelation-contraction continued for many minutes in M-phase extract, up to 6 hours in some cases, suggesting that some components of the wave are recycled. The energy required presumably comes from ATP that is synthesized continuously from endogenous energy stores (Niethammer et al., 2008). The periodic behavior was observed in different geometries (semi-spherical drops, flattened drops, square drops and cylinders) and when the extract was in contact with different materials (untreated glass, glass coated with poly-lysine, glass passivated by silanization, oil and air). Similar waves were observed in concentrated lysates from mitosis-arrested HeLa cells (supplementary material Fig. S1), suggesting that periodic gelation-contraction in mitotic extracts is a conserved phenomenon.

To test whether inwards movement of the gel was driven by circumferential contraction of a ring of F-actin at the outer edge of the gel or by isotropic contraction of the whole gel, we followed contraction of more complicated shapes that included concavities at their edges. Contraction of a ring at the edge would presumably straighten sharp corners and concavities. Fig. 1F shows an example of gelation-contraction in a rectangular chamber, where three air bubbles created concavities at the edge (chevrons). Note that the gel maintains its shape as it contracts. Similar shape maintenance was seen in other geometries. These data suggest contraction is isotropic.

F-actin organization in the contracting gel

We tested a number of fluorescent probes to visualize actin during gelation-contraction: directly labeled actin monomer (Fig. 2A), low concentrations of rhodamine–phalloidin (not shown), fluorescein-labeled Lifeact peptide (Riedl et al., 2008) (Fig. 2B,C) and GFP–Utrophin (GFP fused to an artificial dimer of the actin-binding domain of Utrophin) (Burkel et al., 2007) (Fig. 3B). Essentially similar behavior was seen with all probes, and contractile wave kinetics imaged at low magnification were similar for dark-field and fluorescent actin probes. The actin monomer probe gave low-contrast images of the waves (Fig. 2A), presumably owing to the high concentration of unpolymerized actin in *Xenopus* egg extracts (Rosenblatt et al., 1997). Using this probe, it was evident that actin concentrated in the contracting gel, but that much of the monomer remained outside the gel. Fig. 2B shows wave 1 and wave 3 of a contracting gel containing 1 μM fluorescein–Lifeact peptide imaged by wide-field fluorescence with a 20× objective in a sandwich format. The white arrows indicate the direction of contraction. Note the dense actin meshwork in the first wave and the sparser meshwork in the third wave. The outer

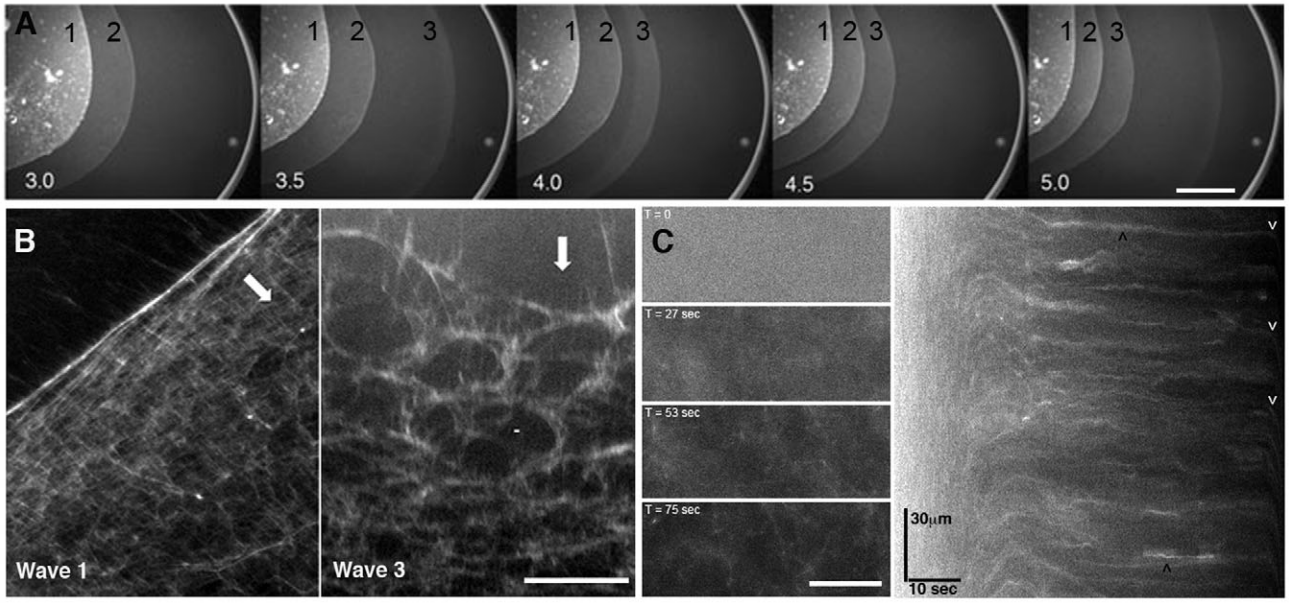

Fig. 2. F-actin organization during gelation-contraction. (**A**) M-phase extract containing 0.3 μM actin labeled with tetramethylrhodamine on lysine residues (Kueh et al., 2008) imaged in sandwich format. The black numbers at the top refer to different waves of gelation-contraction. The white numbers indicate time (in minutes) at room temperature. (**B**) F-actin organization in the wave 1 and wave 3 of a M-phase extract imaged in sandwich format with fluorecin–Lifeact. White arrows indicate the direction of contraction. (**C**) A later wave in the same sample as in B imaged at higher magnification. The panels on the left-hand side are portions from four different frames of a time-lapse movie. The time (T) of image acquisition is shown in white. The panel on the right-hand side is a kymograph presentation of the entire time-lapse movie (in the same orientation as Fig. 1E). Black arrowheads indicate stationary cables of F-actin. White arrowheads indicate the time when contraction of the gel starts. All times are time elapsed from warming room temperature in minutes. Scale bars: 500 μm (A); 15 μm (B); 30 μm (C).

edge of the contracting gel was typically demarcated by a bright line, indicating greater F-actin density. Elsewhere, actin filaments were organized into interconnected bundles, apparently without a preferred orientation. This lack of F-actin orientation is consistent with isotropic contraction of the network. Similar images were obtained with low concentrations of rhodamine–phalloidin (data not shown) and GFP–Utrophin (data not shown).

Using the Lifeact probe, we are able to gain hints to the origin of periodic behavior. The left-hand panels of Fig. 2C show successive images of the same region during the formation of a later wave; T=0 indicates the time immediately after the previous wave had passed by. As time progresses the fluorescence becomes more structured, indicating progressive assembly and/or crosslinking of F-actin bundles. The right-hand panel of Fig. 2C shows a kymograph through the same wave, oriented as in Fig. 1E, with the time axis horizontal and distance axis vertical. On the left (earliest time) the fluorescence is diffuse. At later times (proceeding to the right) it becomes progressively more structured, and bundles seem to grow in thickness (black chevrons). At the last time-points the entire gel undergoes rapid coordinated inward movement (white chevrons). The gel moves very fast once contraction starts and also tended to change in focal plane at this time point, which made it difficult to follow individual bundles during contraction. These images suggest that actin undergoes assembly and/or cross-linking during the non-moving period between each successive wave of inward movement.

Gelation-contraction is cell cycle regulated

To test cell cycle dependence of gelation-contraction, I-phase extracts were prepared by two methods: (i) intact eggs were released from cytostatic factor (CSF) arrest, by treatment with Ca^{2+} ionophore, before extract preparation; and (ii) 400 μM Ca^{2+} was added to M-phase extracts to breakdown CSF, followed by incubation for 30 minutes at 20°C to allow the cell cycle to progress. The added Ca^{2+} is rapidly sequestered into endoplasmic reticulum (ER) in the extract, so this treatment resembles the Ca^{2+} transient during natural fertilization (Desai et al., 1999). In both methods cychoheximide (2 μg/ml) was added to prevent Cyclin B synthesis and re-entry into mitosis. I-phase extracts prepared by either method did not undergo gelation-contraction. Fig. 3A1,A2 shows M-phase and I-phase extracts (made with the Ca^{2+} addition method) that have been placed in Teflon tubing and incubated at room temperature for 26 minutes. Note contraction in the M- but not the I-phase extract. Approximately 4 minutes later the cylinders of extract in these tubes were extruded into a physiological buffer (CSF-XB) (Desai et al., 1999). For the M-phase cylinder, the inner contracted portion remained solid, whereas the outer part dispersed, indicating only the contracted gel is solid. By contrast, the entire I-phase cylinder retained its shape for many minutes after extrusion, suggesting it has gelled, but that the gel has not contracted (Fig. 3A3). Gelation-contraction in M phase, but not I phase, of the same extract preparation was consistently observed (n>20 extract preparations). When cycloheximide was omitted from the I-phase extract, gelation-contraction initiated at 55–70 minutes after shifting to room temperature, presumably corresponding to the entry of the extract into mitosis (data not shown).

F-actin organization in M phase and I phase were compared using the two actin probes fluorescein-labeled Lifeact peptide (Riedl et al., 2008) and GFP–Utrophin (Burkel et al., 2007). Thin squashes were prepared because they inhibited movement of the

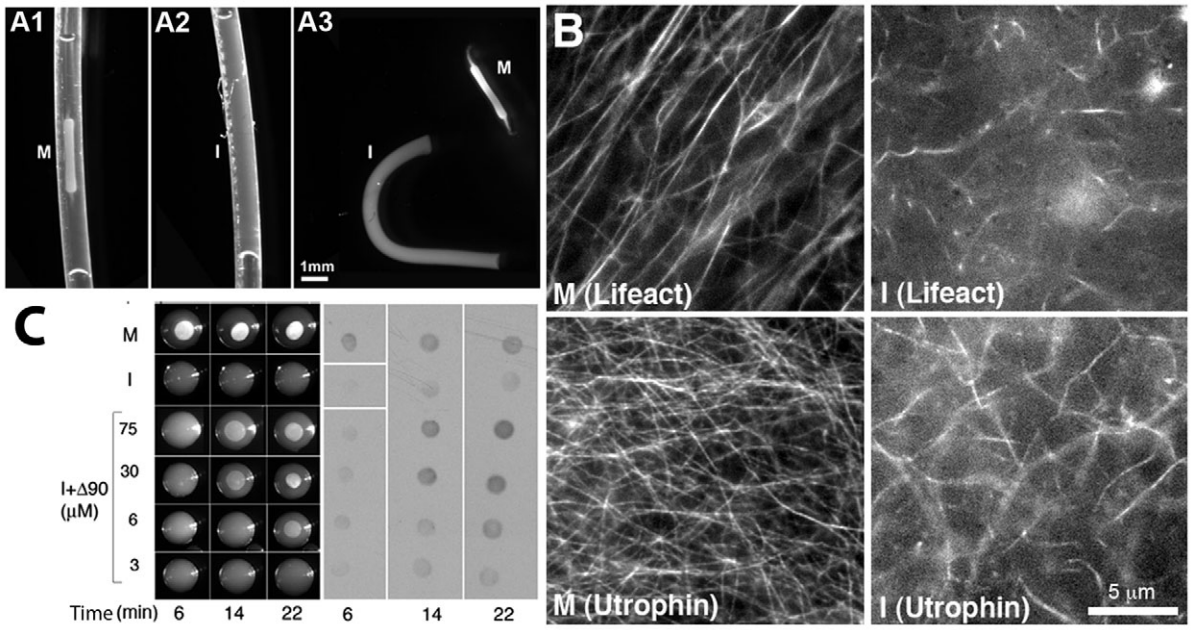

Fig. 3. Gelation-contraction is cell cycle regulated in egg extract. (**A**) M-phase and I-phase extracts were incubated in Teflon tubing and, later, extruded into the physiological buffer CSF-XB (Desai et al., 1999). A1, A2: extracts at 26 minutes after warming to room temperature (dark-field imaging). Note gelation-contraction in the M-phase, but not the I-phase, tube. A3: the same extracts were extruded into buffer at 32 minutes and imaged ~30 seconds later. The contracted part of the M-phase cylinder remains a solid, while the remainder disperses as a liquid. The entire I-phase cylinder remains gelled for many minutes. (**B**) Actin filaments imaged (100×, wide-field imaging) in M phase or I phase with fluorescein–Lifeact or GFP–Utrophin (as labeled). Note that the bundles are more abundant in M phase. (**C**) Addition of Cyclin B Δ90 to I-phase extract triggers gelation-contraction as imaged in drop format (left-hand panels). Time after warming to room temperature is shown. The dot blots in the right-hand panels are samples from the same extracts collected at the same time points and probed with anti-MPM2 antibody, which binds to phosphorylated Cdk1 epitopes.

actin gel and facilitated imaging. M-phase extract contained abundant thick actin bundles that were obviously organized into a macroscopic gel, whereas I-phase extract contained sparser less-organized bundles (Fig. 3B, compare the M with the I images). The exact appearance of actin bundles varied between positions in the squash, but the observation that bundles were thicker and/or more prevalent in M- rather than I-phase was highly reproducible (n>10 extract preparations, both probes). These data suggest that actin is more polymerized and/or more bundled in M-phase relative to I-phase extract, which presumably contributes to the observed difference in bulk gelation-contraction.

To test whether Cdk1 regulates gelation-contraction, as for other aspects of M phase, we added non-degradable Cyclin B Δ90 to I-phase extracts. This treatment stably activates Cdk1 (Murray et al., 1989). Increasing concentrations of Cyclin B Δ90 (expressed as a maltose-binding protein fusion) were added to I-phase extract containing cycloheximide. We scored for gelation-contraction (Fig. 3C, left-hand panels), and for Cdk1 activity using a simple dot blot immunoassay with MPM2, a monoclonal antibody that recognizes Cdk1 phosphorylation sites (Ding et al., 1997) (Fig. 3C, right-hand panels). Addition of 6 μM or more of Cyclin B Δ90 restored gelation-contraction to I-phase extracts. The first contraction initiated with a lag time that varied inversely with the amount of Cyclin B Δ90 protein added, for example, 8.5 minutes for 75 μM compared with 16 minutes for 6 μM. Once initiated, contractions were similar to those of M-phase extracts, with multiple waves of gelation-contraction moving inwards (data not shown). MPM2 dot blots showed that gelation-contraction correlated with Cdk1 activity (higher levels give darker spots), both across Cyclin B Δ90 concentration and time delays. These data are consistent with regulation of gelation-contraction by Cdk1 activity.

A role for Arp2/3 nucleation in gelation-contraction activity?

Bulk gelation-contraction is a complex behavior, probably requiring nucleation, elongation, crosslinking and perhaps depolymerization of actin filaments, as well as polymerization and activity of myosin II. Any of these steps could be cell cycle regulated. To probe possible regulatory mechanisms we first added *Listeria* monocytogenes to the extracts (Theriot et al., 1994). *Listeria* comet-tail assembly requires Arp2/3-catalyzed nucleation, filament elongation and crosslinking but not myosin II activity (Welch et al., 1998; May et al., 1999; Loisel et al., 1999). The length of comet tails provides a measure of the actin disassembly rate (Rosenblatt et al., 1997). Bacteria (visualized with Hoechst dye) were scored for a thick layer of actin surrounding them (cloud) or for a comet of actin extending behind them (tail). The frequency of clouds and tail formation were much higher in M phase (Fig. 4). Clouds were rarely observed in I phase, and the few tails formed contained much less F-actin than those in M phase; these differences were reproduced in six separate extract preparations using both methods for making the I-phase extract. Movement of the *Listeria* that did assemble tails was observed in both M phase and I phase but I-phase movement was less persistent, with bacteria often appearing to separate from their weak tails; however, movement was faster (on average) in I-phase extracts [14 μm/minute (n=4)], than in M-phase extracts [8.6 μm/minute (n=12)]. The fast movement rate of the *Listeria* that did assemble tails in I-phase suggests that the concentration of polymerizable actin monomer cannot be much lower in I phase compared with that in M phase. Overall, these data suggest that Arp2/3 is either more active in M phase than in I phase or that it is more readily recruited to actin monomers in M phase.

Regulation of myosin II activity

Myosin II generates force for gelation-contraction in *Xenopus* egg extracts (from immuno-depletion data) (Bendix et al., 2008). To test whether myosin II is cell cycle regulated in bulk extract, we first measured phosphorylation of myosin regulatory light chain (MRLC) on S19 by immunoblotting (Matsumura et al., 1998). S19 was phosphorylated in both M phase and I phase. This experiment was repeated several times and in some repeats light chain phosphorylation was up to ~2 times higher in M phase (Fig. 5A) in others there was less or no difference (data not shown). According to this assay myosin II might be somewhat more active in M phase rather than in I phase, but this modest difference seems insufficient to explain the all-or-none difference in gelation-contraction.

To test whether myosin II regulation alone determines the difference between gelation-contraction in M phase compared with I phase, we artificially forced additional actin polymerization and bundling by adding phalloidin, a small molecule that promotes filament nucleation and stabilization. We then asked whether the I-phase extract could contract. Addition of phalloidin did not inhibit contraction in M phase and promoted contraction in I phase (Fig. 5B). At the three highest drug concentrations tested (15–150 μM final concentration), gelation-contraction occurred within 120–150

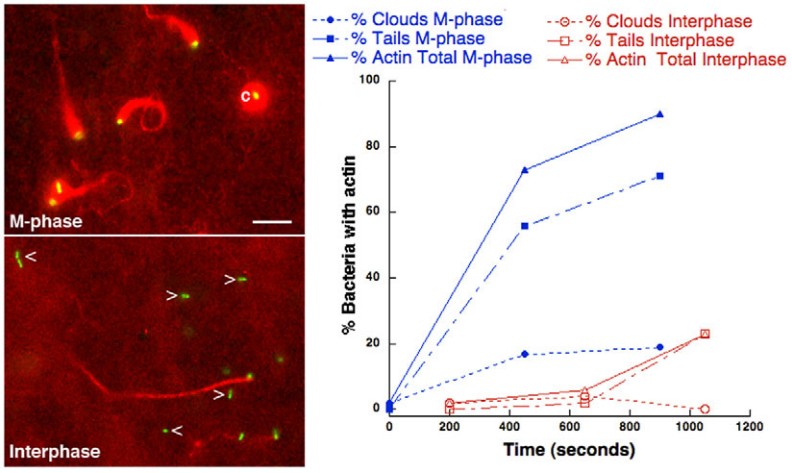

Fig. 4. *Listeria* motility in M- and I-phase *Xenopus* egg extracts. Left-hand panels: Hoechst-stained *Listeria* (green) were added to extracts along with tetramethylrhodamine-labeled actin (red). Images shown are merged frames from time-lapse movies. Note most *Listeria* have robust actin structures; comet tails or clouds (white C) in M phase, whereas in I phase many have no associated actin (white arrowheads). The few tails that assemble in I-phase are thin and contain fewer actin filaments. Some tails are short (bottom right-hand corner) and a few are unusually long. Scale bar: 5 μm. The graph quantifies the percentage of bacteria with associated actin as a function of time after warming to room temperature. Blue solid symbols are M-phase extract and red open symbols are I-phase extract. Total nucleation activity (clouds and tails) are represented by triangles, that by tails with squares and that by clouds with circles.

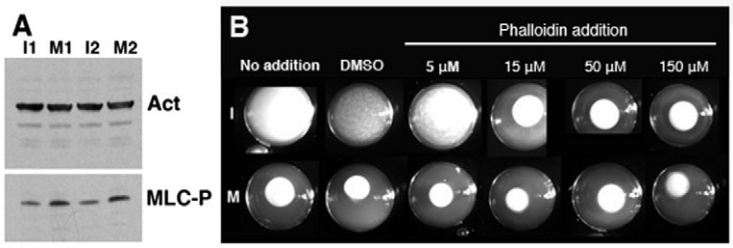

Fig. 5. Cell cycle regulation of myosin II activity. (**A**) Western blot probing two different M-phase and I-phase extract pairs with an antibody against phosphorylated myosin light chain (MLC-P). For a loading control, the blot was also probed with a monoclonal antibody against actin (Act). (**B**) Addition of phalloidin induces gelation-contraction in I-phase extracts. Phalloidin was added and drops were immediately transferred to room temperature for imaging. The 60-minute time point is shown for each condition. Scale bar: 500 µm.

seconds of warming the I-phase extract, and contraction rates were comparable to those in M-phase extracts. The minimal concentration of phalloidin (15 µM) occasionally promoted several rounds of gelation-contraction in I phase (data not shown). We conclude that differences in myosin II activity alone are not likely to determine differences in M phase compared with I phase in gelation-contraction given that forcing polymerization also forces contraction.

Regulation of actin depolymerization

Gelation-contraction could also be cell cycle regulated at the level of actin depolymerization, as there is evidence that the central actin depolymerization factor cofilin is cell cycle regulated in *Xenopus* and other vertebrate systems (Abe et al., 1996; Amano et al., 2002; Kaji et al., 2003). To test this, we measured the rate of depolymerization of fluorescently labeled actin filaments elongated from fragments of *Limulus* acrosomal processes (Kueh et al., 2008). Both M- and I-phase extracts exhibited robust depolymerization activity. I-phase extract was ~2 times more active in depolymerization ($t_{1/2}$≈20 seconds) compared with that of M-phase extract ($t_{1/2}$≈40 sec) (Fig. 6A,B).

Cofilin is negatively regulated by phosphorylation on S3 (Agnew et al., 1995). We performed western blots with an antibody to this phosphorylation site and found higher phosphorylation in M phase than in I phase (Fig. 6C), consistent with previous work (Abe et al., 1996; Amano et al., 2002; Kaji et al., 2003). However, when we added Cyclin B Δ90, in amounts that restored gelation-contraction and increased detection of MPM2 epitopes there was no concomitant increase in cofilin phosphorylation (Fig. 6C; see also Fig. 3C). This experiment uncoupled change in cofilin phosphorylation from change in contractility. It is thus unlikely that regulation of cofilin depolymerization activity is crucial for cell cycle regulation of bulk gelation-contraction in our system, although it might well be important in vivo.

Live actin imaging in zebrafish embryos

To ask whether actin polymerization in bulk cytoplasm is cell cycle regulated in living embryos, we turned to transparent zebrafish embryos. Cell-cycle-regulated microtubule dynamics are similar in early *Xenopus* and zebrafish embryos (Wühr et al., 2010), and we reasoned the same might be true for actin. Zebrafish zygotes, ~30 minutes after fertilization, were injected with Alexa-Fluor-647-conjugated Tubulin, as an indicator of cell cycle state and the GFP–Utrophin probe, to visualize filamentous actin (Burkel et al., 2007). Live image sequences were collected starting at the two-cell stage using a laser confocal microscope and a 20× objective.

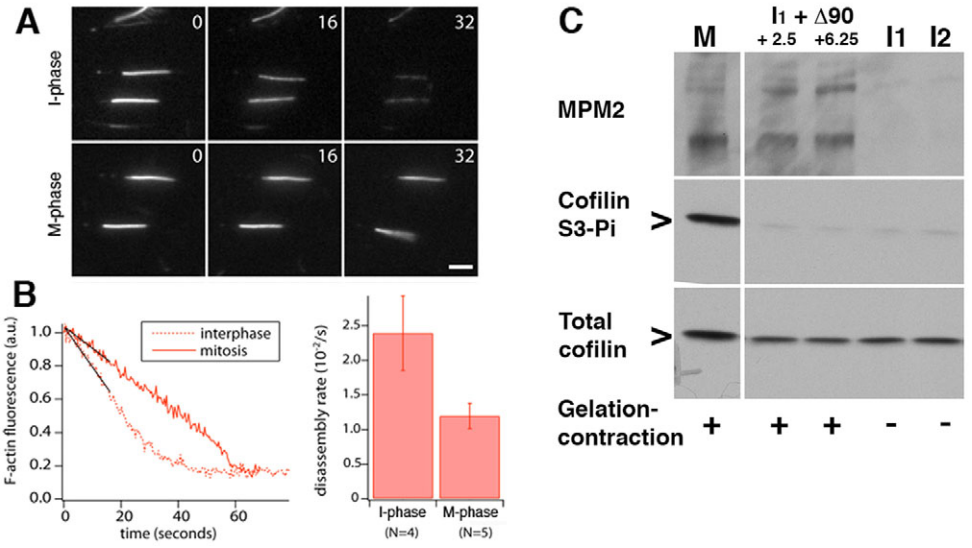

Fig. 6. Cell cycle regulation of actin depolymerization. (**A**) Fluorescent F-actin bundles were grown off of acrosome fragments in perfusion chambers, extract (I or M phase) was then perfused in and the depolymerization rate was quantified by imaging (Kueh et al., 2008). Three different frames from time-lapse movies are shown. White numbers indicate time after extract perfusion in seconds. Scale bar: 2 µm. (**B**) Quantification of depolymerization rates. The left-hand graph is a timecourse of depolymerization from two bundles (one bundle from each extract type). The right-hand bar graph gives the average depolymerization, measured on multiple bundles from the indicated number of independent experiments (N). (**C**) Western blot for cell cycle state (with anti-MPM2 antibody) and cofilin activity [anti-cofilin-S3-*P* (inactive cofilin)]. Lanes are as follows: M, M-phase extract; I1 and I2, two different I-phase extracts; I1 + Δ 90, I-phase extract 1 with MBP–Cyclin B Δ90 added (to 2.5 and 6.25 µM final concentration).

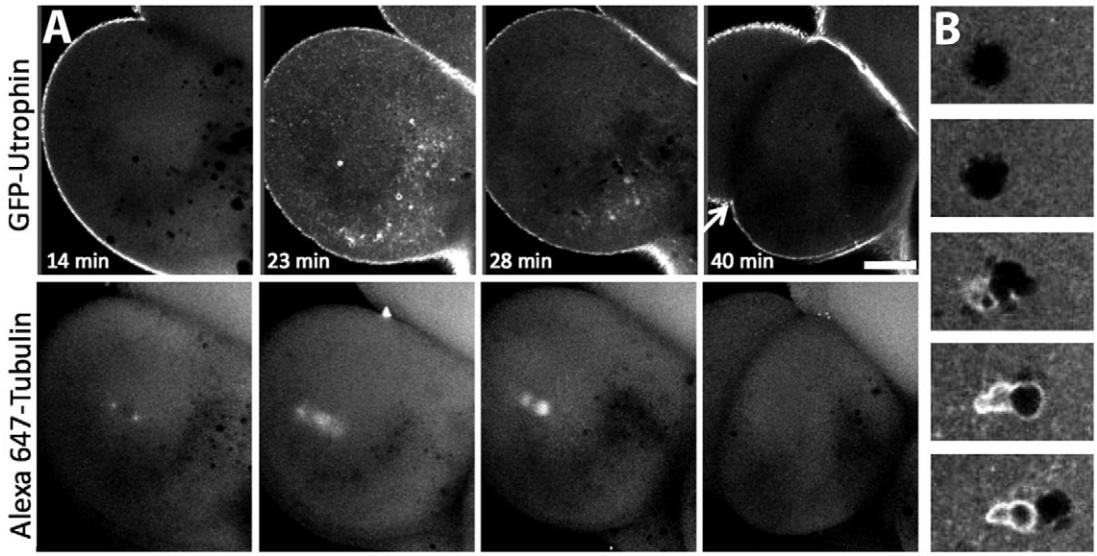

Fig. 7. Cell-cycle-regulated actin assembly in zebrafish blastomeres. (**A**) A zebrafish embryo injected with the F-actin marker GFP–Utrophin (top frames) and Alexa-Fluor-647–Tubulin (bottom frames). Imaging was started at the two-cell to four-cell transition (t=0 minutes). At 14 minutes, the nuclear envelope has not broken down (it excludes the tubulin label), indicating prophase. The cortex, but not the cytoplasm, is strongly labeled with GFP–Utrophin. At 23 minutes, the spindle has formed, indicating metaphase. GFP–Utrophin signal in the cytoplasm is strong, especially around vesicles. Vesicles with GFP–Utrophin comet tails begin to move (supplementary material Movie 2). At 28 minutes, the poles of the spindle move apart (anaphase) and much of the cytoplasmic GFP–Utrophin signal disappears. Vesicle movement ceases (supplementary material Movie 2). At 40 minutes, an indentation on cortex indicates start of cytokinesis (white arrow) and the cytoplasmic GFP–Utrophin signal has largely disappeared. Scale bar: 50 μm. (**B**) Higher magnification of vesicle movement during mitosis visualized with GFP–Utrophin (4× that in shown in A). The top panel is at t=18 minutes (same start time as in A). The time between each panel is 48 seconds. The vesicle (i.e. the area where label is excluded) initially appears static, but then starts moving away from polymerizing actin.

During prophase, before nuclear envelope breakdown, the Utrophin probe localized strongly to the cortex and showed weak diffuse localization in the cytoplasm (Fig. 7A, 14 minutes). At 23 minutes in this sequence, the mitotic spindle assembled, indicating metaphase; at this time-point the GFP–Utrophin signal was stronger in the cytoplasm, where it was mainly localized around vesicles of different sizes, in some cases extending into comet-tail like structures (Fig. 7A, 23 minutes; Fig. 7B). Many of the vesicles moved within the cytoplasm (supplementary material Movie 2). Addition of small molecules demonstrated that the movement of vesicles was dependent upon the actin cytoskeleton and not microtubules (data not shown). As the blastomere progressed into anaphase, the Utrophin signal in the cytoplasm decreased and became very low during cytokinesis, when cleavage furrow staining becomes evident at the cortex (Fig. 7A, 40 minutes, arrow). Vesicle movement also ceased at this time. This cycle of F-actin buildup around vesicles deep into the cytoplasm during metaphase, and the decrease during anaphase, repeated in the next cell cycle (supplementary material Movie 2). We observed cyclic accumulation of F-actin assemblies and vesicle movement in cytoplasm, peaking during mid-mitosis in multiple blastomeres. We conclude that actin polymerization around vesicles in embryonic cytoplasm is regulated by the cell cycle, with a peak in mid-mitosis, consistent with our extract observations. Possible functions of this mitotic actin polymer are discussed below.

Discussion

Gelation-contraction in cell extracts was one of the founding observations for the biochemistry of cell motility (Kane, 1976; Pollard, 1976; Condeelis et al., 1977; Clark and Merriam, 1978). The gelation-contraction we report on here occurs much more rapidly than in the classic work, presumably because we used essentially undiluted mitotic cytoplasm, compared with the high-speed supernatants used in most older studies. Periodic contractility was reported once before in extracts, in a study that used high-speed supernatants and required hyperphosphorylation by (non hydrolyzable) ATPγS (Ezzel et al., 1983). To our knowledge, cell cycle regulation of gelation-contraction has not been reported previously. Formation of Arp2/3-dependent actin comet tails around vesicles during prophase and metaphase, but not interphase, was recently reported in *C. elegans* zygotes, using GFP–moesin as a probe (Verlarde et al., 2007). Thus the cell cycle regulation we see in *Xenopus* extract and zebrafish embryos might be conserved. Although the precise implications of our observations for intact egg or embryo biology remain to be determined, they draw attention to the under-studied problem of actomyosin behavior in bulk cytoplasm and provide a system for investigating its biophysics and regulation.

Origin of periodicity

It is not clear that periodic gelation-contraction occurs in living embryos. However, the dramatic highly regular periodicity of contractility in M-phase extracts is an interesting biophysical phenomenon that might reveal new mechanistic principles. We considered two models for periodicity. First, stick-slip dynamics, in which stress in the gel is generated by contraction and builds up to a critical level that detaches the gel from the coverslip. Gel movement then dissipates the stored stress, leading to periodic behavior. This origin of periodic behavior has been proposed for contractility in *Drosophila* embryo epithelial cells (Martin et al., 2009). We have not ruled it out, but we do not favor it because the time between successive waves was similar in several different

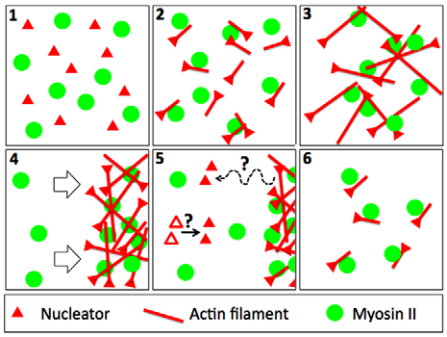

Fig. 8. Model for periodic gelation-contraction. (1) Nucleators (possibly activated Arp2/3) and myosin II are initially homogeneous. (2) Actin filaments start to elongate. For ~90 seconds they are too short to interact. (3) Filaments elongate sufficiently that they interact through myosin II (and possibly other crosslinkers; not shown), initiating rapid contraction. (4) Gel contraction sweeps F-actin and nucleators inwards (arrows), temporarily depleting nucleators outside the gel (but not myosin II or G actin; not shown). (5) Nucleators are replaced outside the gel. Possible replacement mechanisms (indicated by the '?') include continuous activation from an inactive pool (open triangles) and recycling from the contracting gel (dotted line). (6) The cycle re-initiates.

observation geometries (Fig. 1B) and was unaffected by passivating the glass surface in various ways (data not shown). Second, we considered a gel growth model (Fig. 8), in which actin filaments continuously nucleate and elongate, and must achieve a critical length and/or density to allow crosslinking and contraction by myosin II. The contraction clears out long actin filaments, but leaves behind nucleating sites for a subsequent round of assembly. This model is more consistent with all our data.

Cell-cycle regulation by actin nucleation?

We saw longer more organized F-actin bundles in M phase than in I phase (Fig. 3B), suggesting that either more polymer or more bundling occurs in M phase. *Listeria* comet tail assembly, but not comet tail elongation rate, was higher in M phase than in I phase (Fig. 4), and comet tails were more prevalent around endogenous vesicles in M phase than in I phase in zebrafish (Fig. 7), as found previously for nematode (Verlarde et al., 2007) blastomeres. Myosin II (Fig. 5) and cofilin activities (Fig. 6) are both cell cycle regulated to some extent, but these steps do not seem to be crucial for regulating the bulk behavior. Together, these data suggest that Arp2/3 is more active in M phase, or more readily recruited to nucleation sites, and that regulation of this activity is the most crucial for regulation of bulk behavior.

We invested considerable effort in characterizing the molecular mechanism of the nucleation that drives bulk gelation-contraction, but so far our data are inconclusive. As a direct test of the role of Arp2/3, we added the CA domain of scar1 (amino acids 522–559) to M-phase extracts. This peptide can inhibit Arp2/3 activity in vitro (May et al., 1999; Brieher et al., 2004). We observed partial inhibition of gelation-contraction (data not shown), consistent with a role of Arp2/3, but we consider the data inconclusive because high concentrations of peptide were required and we lack a strong control for non-specific effects of the peptide. Our imaging in zebrafish revealed that some, and perhaps most, of the cytoplasmic F-actin that assembles during mitosis is associated with vesicles, either as a rim or a comet-tail. These images are consistent with Arp2/3-nucleated polymerization at the surface of vesicles in the extract (Taunton et al., 2000). Similar actin comet tail assembly in prophase and metaphase *C. elegans* embryos requires Cdc42 and Arp2 (Verlade et al., 2007), consistent with higher Arp2/3 activity during M phase in early embryos.

One area of possible regulation that we did not explore systematically was cell cycle regulation of bundling and/or crosslinking factors. We investigated this question at the suggestion of a reviewer. We added fairly high concentrations (up to 2 μM) of three different cross-linking proteins (fimbrin, α-actinin and tropomyosin) to I-phase extracts. We saw no enhancement of bulk gelation-contraction with the addition of any of the proteins and there was no evidence for additional bundling in high-magnification images with the α-actin in addition (data not shown). It was not clear from these data whether the concentrations added were insufficient to induce extra bundling, whether the system is already saturated with bundling factors or whether the added proteins come under endogenous regulation, which inhibits their activity. Phalloidin, which forced gelation-contraction in I phase, also dramatically increased bundling, as observed in high-magnification images (data not shown), so the two processes could be correlated, but in general it will be hard to separate effects on F-actin concentration and/or stability from effects on bundling.

Possible functions of cytoplasmic F-actin during mitosis

We do not interpret our data as suggesting that periodic gelation-contraction occurs during M phase in embryos. We do, however, think it supports the idea that embryos polymerize more actin in the bulk cytoplasm in M phase than in I phase. We considered three non-exclusive possibilities for the probable functions of this M-phase actin: (i) vesicle trafficking, (ii) mitotic spindle assembly, and (iii) mechanics of the bulk cytoplasm. Regarding the first possibility, formation of actin comet tails on endosomes correlates with massive waves of exocytosis and endocytosis that follow fertilization in *Xenopus* (Taunton et al., 2000), and exocytosis is decreased during mitosis in tissue culture cells (Boucrot and Kirchhausen, 2007). Perhaps actin polymerization around endosomes decreases exocytosis during M phase in embryos, and loss of this inhibition promotes exocytosis during cytokinesis. In the second possibility, mitotic F-actin, working together with myosin II or myosin X, could promote spindle assembly (Rosenblatt et al., 2004; Cytrynbaum et al., 2005; Woolner et al., 2008). Consistent with this view, a contractile actin meshwork facilitates chromosome congression in starfish meiosis (Lenart et al., 2005). In the third scenario, actin polymerization during mitosis might serve to physically stiffen the cytoplasm to hold the centrosomes in place. In early *Xenopus* and zebrafish embryos, astral microtubules at metaphase are too short to position and orient the mitotic spindle for the first few cell cycles (Wühr et al., 2009). Instead, the spindle assembles in a position and orientation that is pre-defined by the positions of the centrosomes at prophase. Centrosomes are positioned during the previous I phase, by pulling forces on the much longer I-phase astral microtubules (Wühr et al., 2010). Stiffening of the cytoplasm in M phase could help hold the centrosomes in place during spindle assembly, whereas softening in I phase could promote centrosome movement. More speculatively, local softening in the cleavage plane could help guide furrow ingression. Intact *Xenopus* eggs undergo cell-cycle-regulated stiffening (Hara et al., 1980), which was attributed to waves of cortical contraction (Rankin and Kirschner, 1997), but stiffening of bulk cytoplasm might also contribute. Using micro-dissection and physical manipulation, Elinson (Elinson, 1983)

noted that both the cortex and the bulk cytoplasm undergo cell-cycle-regulated change in physical properties. Drug treatments revealed than some of these were due to actin (and presumably myosin II) and some due to microtubules.

The importance of cortical actomyosin in shaping cells and embryos is widely accepted, and many studies have documented how it is regulated by the cell cycle, especially during cleavage. Internal actomyosin has long been known to exist, but it has been much less studied, and its functions are less clear. Our work shows that the bulk cytoplasmic pool of actomyosin undergoes dramatic cell-cycle-regulated change in organization, suggesting it too contributes to shaping cells, and/or organizing their internal contents, in a cell-cycle-regulated manner. More work is required to elucidate the molecular mechanisms by which this bulk pool is regulated by the cell cycle and to test its functions. Actomyosin in the bulk cytoplasm might be especially important in large eggs and blastomeres, where the mitotic spindle is a long way from the cortex, but it deserves more attention in all cells.

Materials and Methods

Xenopus egg extract

M-phase ('CSF') extract was prepared as described previously (Desai et al., 1999), except that cytochalasin D was omitted from all steps and the crushing spin was run at 4°C instead of 16°C. I-phase extracts were prepared using two methods that cause a transient increase in Ca^{2+} that mimics fertilization. In method 1, de-jellied eggs were activated with 0.2 µg/ml A23187 (Sigma) for 5–7.5 minutes and washed in XB (Valentine et al., 2005) before extract preparation. In method 2, $CaCl_2$ was added to CSF extract to a final concentration of 0.4 mM (Desai et al., 1999), and the extract was incubated at room temperature for 30 minutes. For both methods, 2 µg/ml cycloheximide was usually added to the extract to prevent re-entry into mitosis. To freeze extract, we first added an energy mix (30 mM creatine phosphate, 1 mM ATP and 1 mM $MgCl_2$; final concentrations) and sucrose (50 mM; final concentration), froze small aliquots in liquid nitrogen and stored at –80°C. Cell-cycle-regulated gelation-contraction was stable for at least 2 months.

Assessment of cell cycle state by MPM2 immunoreactivity

Western blots were performed with MPM2 (antibody #05-368, Upstate). Many strong bands were seen in M phase but not I phase, as expected. For experiments with many samples (Fig. 3) we used dot bots. Aliquots were diluted 1:10 with CSF-XB, 1 µl was spotted onto nitrocellulose and air-dried.

Concentrated M-phase extracts (from HeLa cells)

Extracts were prepared from *S*-trityl L-cysteine (Sigma–Aldrich) arrested HeLa S3 cells grown in suspension, as described previously (Chang et al., 2009), but without latrunculin A. Protein concentration was typically 10–15 mg/ml.

Microscopy

The drop format microscopy was performed with 1 µl drops of extract deposited onto a poly-lysine-coated coverslip on the bottom of a petri dish containing mineral oil. Drops were side-illuminated and imaged with a dissecting microscope. The sealed chamber (sandwich format) microscopy was performed with 3–4 µl of extract was sandwiched between two glass cover slips, surrounded with a shim of moist Whatman #1 filter paper or spacers made from #1.5 cover slips. Chambers were sealed with VALAP (1:1:1 mixture of wax, Vaseline and lanolin). Rectangular chambers (Fig. 2F) were cut out from parafilm, blocked with 0.2% casein and dried before extract addition. The tube and capillary format microscopy were performed by inserting extract in a glass capillary tube or section of teflon tubing. It was imaged using a dissecting microscope in the tube or after extrusion into buffer.

Listeria motility assays

Iodoacetate-killed *Listeria* were incubated 4°C for 30 minutes with extracts containing trace (0.3 µM) tetramethylrhodamine actin and 0.3 µM Hoechst dye (Sigma B2261). This long pre-incubation is required for *Listeria* motility in *Xenopus* extracts for unknown reasons (Theriot and Fung, 1998). 5 µl drops of extract were sealed between a slide and an 18-mm^2 coverslip using VALAP. These thin squashes did not exhibit gelation-contraction.

Actin depolymerization assays

These assays were performed as described previously (Kueh et al., 2008).

Zebrafish imaging

Zebrafish embryos were injected ~30 minutes after fertilization. The injection site was in the yolk but close to the cell. Tubulin was injected first [~1 nl of a 11 mg/ml Alexa-Fluor-647-labeled stock (labeling ratio 0.7) in 50 mM potassium glutamate, 0.5 mM $MgCl_2$, 50 mM sucrose, pH 7]. Then GFP–Utrophin was injected at nearby site (~1 nl of a 1 mg/ml stock in 150 mM aspartic acid, 10 mM HEPES solution pH 7.2–7.3). For imaging, embryos were selected on the basis of their ability to cleave and were then mounted with a mold made out of agarose. Imaging was performed on a Zeiss LSM 710 microscope with 20× water immersion objective (NA 1.0). Images were taken every 24 seconds, at three *z*-planes (21 µm between each plane). For Fig. 7 and supplementary material Movie 2, the three tubulin planes were projected and combined with the middle section for the Utrophin channel. All animal experiments were performed according to the procedures defined by the Animal Care and Use Committee of Harvard Medical School.

This work was supported by NIH GM023928. Early experiments were piloted by MBL Woods Hole Physiology Course students in 2006–2008. The MBP–Cyclin B Δ90 construct was a gift of Adrian Salic (HMS) and was expressed by Aaron Groen (HMS). Bill Brieher (U Illinois) provided labeled actin, actin binding/bundling proteins and valuable discussion. Paul Chang (MIT) and Aaron Groen provided HeLa cells and guidance on making concentrated extracts. Dyche Mullins (UCSF) provided the CA domain of scar1. David Burgess (Boston College) provided GFP–Utrophin. Sean Megason (HMS) helped with zebrafish husbandry and imaging. C.M.F. thanks Marc Kirschner for tolerance, support and happy frogs. Deposited in PMC for release after 6 months.

Supplementary material available online at
http://jcs.biologists.org/cgi/content/full/124/12/2086/DC1

References

Abe, H., Obinata, T., Minamide, L. and Bamburg, J. R. (1996). Xenopus laevis actin-depolymerizing factor/Cofilin: a phosphorylation-regulated protein essential for development. *J. Cell Biol.* **132**, 871-885.

Agnew, B. J., Minamide, L. S. and Bamburg, J. R. (1995). Reactivation of phosphorylated actin depolymerization factor and identification of the regulatory site. *J. Biol. Chem.* **270**, 17582-17587.

Amano, T., Kaji, N., Ohashi, K. and Mizuno, K. (2002). Mitosis-specific activation of LIM motif-containing protein kinase and roles of cofilin phosphorylation and dephosphorylation in mitosis. *J. Biol. Chem.* **277**, 22093-22102.

Belmont, L. D., Hyman, A. A., Sawin, K. E. and Mitchison, T. J. (1990). Real time visualization of cell cycle-dependent changes in microtubule dynamics in cytoplasmic extracts. *Cell* **62**, 579-589.

Bendix, P. M., Koenderink, G. H., Cuvelier, D., Dogic, Z., Koeleman, B. N., Brieher, W. M., Field, C. M., Mahadevan, L. and Weitz, D. A. (2008). A quantitative analysis of contractility in active cytoskeletal protein networks. *Biophys. J.* **94**, 3126-3136.

Boucrot, E. and Kirchhausen, T. (2007). Endosomal recycling controls plasma membrane area during mitosis. *Proc. Natl. Acad. Sci. USA* **104**, 7939-7944.

Bray, D. and White, J. G. (1988). Cortical flow in animal cells. *Science* **239**, 883-888.

Brieher, W. M., Coughlin, M. and Mitchison, T. J. (2004). Fascin-mediated propulsion of Listeria monocytogenes independent of frequent nucleation by the Arp2/3 complex. *J. Cell Biol.* **165**, 233-242.

Burkel, B. M., von Dassow, G. and Bement, W. M. (2007). Versatile fluorescent probes for actin filaments based on the actin-binding domain of utrophin. *Cell Motil. Cytoskeleton* **64**, 822-832.

Chang, P., Coughlin, M. and Mitchison, T. J. (2009). Interaction between Poly (ADP-ribose and NuMA contributes to mitotic spindle pole assembly. *Mol. Biol. Cell* **20**, 4575-4585.

Clark, T. G. and Merriam, R. W. (1978). Actin in Xenopus oocytes I. Polymerization and gelation *in vitro*. *J. Cell Biol.* **77**, 427-438.

Condeelis, J. S. and Taylor, D. L. (1977). The contractile basis of amoeboid movement. V. The control of gelation, solation, and contraction in extracts from Dictyostelium discoideum. *J. Cell Biol.* **74**, 901-927.

Cytrynbaum, E. N., Sommi, P., Brust-Mascher, I., Scholey, J. M. and Mogilner, A. (2005). Early spindle assembly in Drosophila embryos: role of a force balance involving cytoskeletal dynamics and nuclear mechanics. *Mol. Biol. Cell* **16**, 4967-4981.

Dao, V. T., Dupuy, A. G., Gavet, O., Caron, E. and de Gunzburg, J. (2009). Dynamic changes in Rap1 activity are required for cell retraction and spreading during mitosis. *J. Cell Sci.* **122**, 2996-3004.

Desai, A., Murray, A. W., Mitchison, T. J. and Walczak, C. E. (1999). The use of Xenopus egg extracts to study mitotic spindle assembly and function in vitro. *Methods Cell Biol.* **61**, 385-412.

Ding, M., Feng, Y. and Vandre, D. D. (1997). A partial characterization of the MPM-2 phosphoepitope. *Exp. Cell Res.* **231**, 3-13.

Eggert, U. S., Mitchison, T. J. and Field, C. M. (2006). Animal cytokinesis: from parts list to mechanisms. *Annu. Rev. Biochem.* **75**, 543-566.

Elinson, R. P. (1983). Cytoplasmic phases in the first cell cycle of the activated frog egg. *Dev. Biol.* **100**, 440-451.

Ezzell, R. M., Brothers, A. J. and Cande, W. Z. (1983). Phosphorylation-dependent contraction of actomyosin gels from amphibian eggs. *Nature* **306**, 620-622.

Gibson, M. C., Patel, A. B., Nagpal, R. and Perrimon, N. (2006). The emergence of geometric order in proliferating metazoan epithelia. *Nature* **442**, 1038-1041.
Hara, K., Tydeman, P. and Kirschner, M. W. (1980). A cytoplasmic clock with the same period as the division cycle in Xenopus eggs. *Proc. Natl. Acad. Sci. USA* **77**, 462-466.
Kaji, N., Ohashi Shuin, M., Niwa, R. and Uemura, T. (2003). Cell cycle-associated changes in slingshot phosphatase activity and roles in cytokinesis in animal cells. *J. Biol. Chem.* **278**, 33450-33455.
Kane, R. E. (1976). Preparation and purification of polymerized actin from sea urchin extracts. *J. Cell Biol.* **66**, 305-315.
Kueh, H. Y., Charras, G. T., Mitchison, T. J. and Brieher, W. M. (2008). Actin disassembly by cofilin, coronin, and Aip1 occurs in bursts and is inhibited by barbed-end cappers. *J. Cell Biol.* **182**, 341-353.
Kunda, P. and Baum, B. (2009). The actin cytoskeleton in spindle assembly and positioning. *Trends Cell Biol.* **19**, 174-179.
Lenart, P., Bacher, C. P., Daigle, N., Hand, A. R., Eils, R., Terasaki, M. and Ellenberg, J. (2005). A contractile nuclear actin network drives chromosome congression in oocytes. *Nature* **436**, 812-818.
Loisel, T. P., Boujemaa, R., Pantaloni, D. and Carlier, M. F. (1999). Reconstitution of actin-based motility of Listeria and Shigella using pure proteins. *Nature* **401**, 613-616.
Maddox, A. S. and Burridge, K. (2003). RhoA is required for cortical retraction and rigidity during mitotic cell rounding. *J. Cell Biol.* **160**, 255-265.
Martin, A. C., Kaschube, M. and Wieschaus, E. F. (2009). Pulsed contractions of an actin-myosin network drive apical constriction. *Nature* **457**, 495-499.
Matsumura, F., Ono, S., Yamakita, Y., Totsukawa, G. and Yamashiro, S. (1998). Specific localization of serine 19 phosphorylated myosin II during cell locomotion and mitosis of cultured cells. *J. Cell Biol.* **140**, 119-129.
May, R. C., Hall, M. E., Higgs, H. N., Pollard, T. D., Chakraborty, T., Wehland, J., Machesky, L. M. and Sechi, A. S. (1999). The Arp2/3 complex is essential for the actin based motility of Listeria monocytogenes. *Curr. Biol.* **9**, 759-762.
Mitchison, J. M. and Swann, M. M. (1955). The mechanical properties of the cell surface. III. The sea-urchin egg from fertilization to cleavage. *Exp. Biol.* **32**, 734-750.
Murray, A. W. and Kirschner, M. W. (1989). Cyclin synthesis drives the early embryonic cell cycle. *Nature* **339**, 275-280.
Murray, A. W., Solomon, M. J. and Kirschner, M. W. (1989). The role of cyclin synthesis and degradation in the control of maturation promoting factor activity. *Nature* **339**, 280-286.
Niethammer, P., Kueh, H. Y. and Mitchison, T. J. (2008). Spatial patterning of metabolism by mitochondria, oxygen, and energy sinks in a model cytoplasm. *Curr. Biol.* **18**, 586-591.
Pollard, T. D. (1976). The role of actin in the temperature-dependent gelation and contraction of extracts of Acanthamoeba. *J. Cell Biol.* **68**, 579-601.
Pollard, T. D. (1981). Cytoplasmic contractile proteins. *J. Cell Biol.* **91**, 156s-165s.
Rankin, S. and Kirschner, M. W. (1997). The surface contractin waves of Xenopus eggs reflect the metachronous cell-cycle state of the cytoplasm. *Curr. Biol.* **7**, 451-454.
Riedl, J., Crevenna, A. H., Kessenbrock, K., Yu, J. H., Neukirchen, D., Bista, M., Bradke, F., Dieter, J., Holak, T. A., Werb, Z. et al. (2008). Lifeact: a versatile marker to visualize F-actin. *Nat. Methods* **5**, 605-607.
Rosenblatt, J., Agnew, B. J., Abe, H., Bamburg, J. H. and Mitchison, T. J. (1997). Xenopus actin depolymerizing factor/cofilin (XAC) is responsible for the turnover of actin filaments in Listeria monocytogenes tails. *J. Cell Biol.* **136**, 1323-1332.
Rosenblatt, J., Cramer, L. P., Baum, B. and McGee, K. (2004). Myosin II-dependent cortical movement is required for centrosome separation and positioning during mitotic spindle assembly. *Cell* **117**, 361-372.
Schroeder, T. E. (1968). Cytokinesis: filaments in the cleavage furrow. *Exp Cell Res.* **53**, 272-276.
Taunton, J., Rowning, B. A., Coughlin, M. L., Wu, M., Moon, R. T., Mitchison, T. J. and Larabelle, C. A. (2000). Actin-dependent propulsion of endosomes and lysosomes by recruitment of N-WASP. *J. Cell Biol.* **148**, 519-530.
Theriot, J. A. and Fung, D. C. (1998). Listeria monocytogenes-based assays for actin assembly factors. *Methods Enzymol.* **298**, 114-122.
Theriot, J. A., Rosenblatt, J., Portnoy, D. A., Goldschmidt-Clermont, P. J. and Mitchison, T. J. (1994). Invovlement of profilin in the actin-based motitlity of L. monocytogenes in cells and in cell-free extracts. *Cell* **76**, 505-517.
Valentine, M. T., Perlman, Z. E., Mitchison, T. J. and Weitz, D. A. (2005). Mechanical properties of Xenopus egg cytoplasmic extracts. *Biophys. J.* **88**, 680-689.
Velarde, N., Gunsalus, K. C. and Piano, F. (2007). Diverse roles for actin in C. elegans early embryogenesis. *BMC Dev. Biol.* **7**, 142.
Verde, F., Dogterom, M., Stelzer, E., Karsanti, E. and Leibler, S. (1992). Control of microtubule dynamics and length by cyclin A- and cyclin B-dependent kinases in Xenopus egg extracts. *J. Cell Biol.* **118**, 1097-1108.
Waterman-Storer, C., Duey, D. Y., Weber, K. L., Keech, J., Cheney, R. E., Salmon, E. D. and Bement, W. M. (2000). Microtubules remodel actomyosin networks in *Xenopus* egg extracts via two mechanisms of F-actin transport. *J. Cell Biol.* **150**, 361-376.
Welch, M. D., Rosenblatt, J., Skoble, J., Portnoy, D. A. and Mitchison, T. J. (1998). Interaction of human Arp2/3 complex and the Listeria monocytogenes ActA protein in actin filament nucleation. *Science* **28**, 105-108.
Woolner, S., O'Brien, L. L., Wiese, C. and Bement, W. M. (2008). Myosin-10 and actin filaments are essential for mitotic spindle function. *J. Cell Biol.* **182**, 77-88.
Wühr, M., Dumont, S., Groen, A. C., Needleman, D. J. and Mitchison, T. J. (2009). How does a millimeter-sized cell find its center? *Cell Cycle* **8**, 1115-1121.
Wühr, M., Tan, E. S., Parker, S. K., Detrich, W. and Mitchison, T. J. (2010). A model for cleavage plane determination in early amphibian and fish embryos. *Curr. Biol.* **20**, 2040-2045.

Journal of Cell Science